

Synthesis and Properties of C_{2h} -Symmetric BN-Heteroacenes Tailored through Aromatic Central Cores

Xinyang Wang,[†] Fan Zhang,^{*,†} Jianhua Gao,[‡] Yubin Fu,^{†,§} Wuxue Zhao,[†] Ruizhi Tang,[†] Wanzheng Zhang,[†] Xiaodong Zhuang,[†] and Xinliang Feng^{†,§}

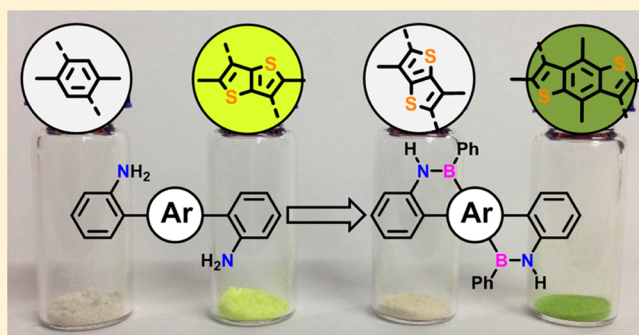
[†]School of Chemistry and Chemical Engineering, State Key Laboratory of Metal Matrix Composites, Shanghai Jiao Tong University, Shanghai 200240, P. R. China

[‡]Key Laboratory of Organosilicon Chemistry and Material Technology of Ministry of Education, Hangzhou Normal University, Hangzhou 311121, P. R. China

[§]Center for Advancing Electronics Dresden (cfaed) and Department of Chemistry and Food Chemistry, Technische Universität Dresden, 01062 Dresden, Germany

S Supporting Information

ABSTRACT: The 2-fold successive electrophilic borylation on one aromatic central core led to a series of C_{2h} -symmetric BN-heteroacenes in excellent yields. For the first time, we introduced trimethylsilyl (TMS) as either leaving group or oriented group for efficiently improving the preparation of BN-embedded polycyclic aromatic hydrocarbons (PAHs). The physical properties of the as-synthesized BN-heteroacenes in either solid state or solution can be finely tuned through the position isomerization or the fused ring numbers of the aromatic central core.



INTRODUCTION

Thanks to their good stability, rich electronic properties, and strong intermolecular interactions, heteroacenes are among the most promising organic semiconductors for application in electronic devices, such as, organic light-emitting diodes (OLEDs), organic solar cells (OSCs), and organic field-effect transistors (OFETs).^{1–3} Full carbon polyacenes with over five fused rings, e.g., hexacene and heptacene etc., are not only air-unstable but chemically labile, readily involved in some chemical reactions such as Diels–Alder-like cycloaddition and homodimerization.^{4,5} Incorporation of heteroatoms into the backbones of polyacenes dramatically improves the chemical and thermal stabilities, as well as essentially tailors the molecular energy levels of the resulting heteroacenes.^{6–8} In this respect, substitution of one or more C=C units by isoelectronic B–N units, offers BN-embedded heteroacenes (denoted as BN-heteroacenes) with remarkable variation in the electronic structures but not geometric structure in comparison with their full carbon analogues.^{9–11} In particular, the different electronegativities of boron and nitrogen atoms in a B–N unit endow the BN-heteroacenes with unique polarities. Accordingly, variation of the relative positions of boron and nitrogen atoms in a BN unit significantly affects the dipole moment of a BN-embedded aromatic compound.^{12–15}

In our previous work, we have reported a series of BN-heteroacenes featuring a *p*-phenylenediamine core fused with versatile aromatic rings in the bilateral sides and explored their

application as the host materials in the device fabrication of blue OLEDs (Figure 1).¹⁶ However, the BN-embedded

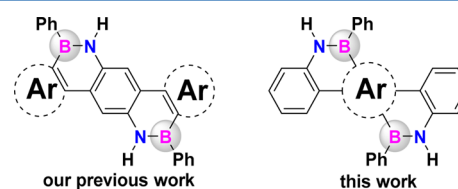
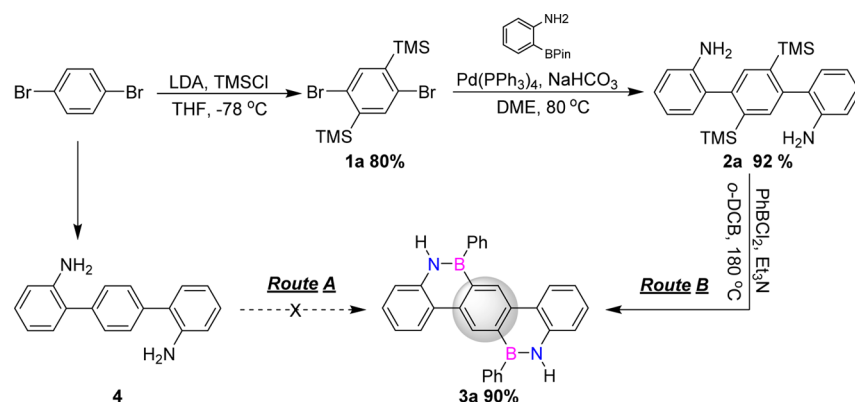


Figure 1. Chemical structures of BN-heteroacenes.

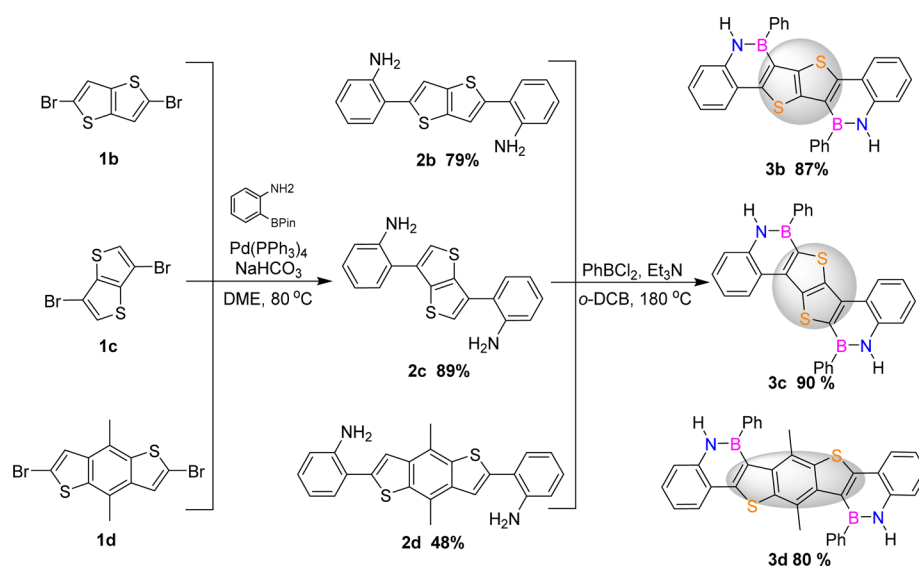
compounds with multiple boron atoms attached on one aromatic unit of the main backbone, have been rarely reported, most probably because multifold electrophilic borylation in one aromatic unit is too sluggish. In 1960, Dewar pioneered the synthesis of 5,9-diphenyl-4,10-diaza-5,9-diborapyrene in a moderate yield of 21% using Friedel–Crafts cyclization of 2,6-biphenyldiamine in the presence of aluminum chloride.¹⁷ It was until very recently that Nakamura and co-workers successfully synthesized BN-embedded hexabenzotetracene in a yield of 32% via a tandem intramolecular electrophilic arene borylation with the help of finely optimized Lewis acid and base additives.¹⁸ Obviously, the lack of the species impedes the

Received: July 28, 2015

Published: September 29, 2015

Scheme 1. Synthetic Routes of BN-Dibenz[*a,h*]anthracene

Scheme 2. Synthesis of BN-Heteroacenes 3b–d



investigation of BN-containing aromatic compounds and their properties and potential applications. With this in mind, our effort is focused on exploring some facile synthetic approaches to achieve new BN-heteroacenes featuring multiboron-attached aromatic central cores.

In this work, we present the concisely synthetic strategies to a new series of C_{2h} -symmetric BN-heteroacenes with various aromatic central cores through the 2-fold electrophilic borylation reaction. We carefully studied the electronic effect of the central cores on the cyclization activity and found that the trimethylsilyl (TMS) group, as either leaving group or oriented group here, can prominently facilitate the attachment of the boron atom at the aromatic unit. The geometric and electronic structures of the as-prepared BN-heteroacenes can be finely tuned through the modification of the aromatic cores, such as position isomerization or the numbers of the fused rings, as indicated by the full characterization including single crystal structure analysis, optical spectroscopy, and electrochemical measurement.

RESULTS AND DISCUSSION

The targeted BN-heteroacenes were synthesized as depicted in Scheme 1 and Scheme 2. To achieve compound 3a, denoted as BN-dibenz[*a,h*]anthracene (BN-DBA), at first, a typical protocol was used through the intermediate compound 4

([1,1':4',1''-terphenyl]-2,2''-diamine). Unfortunately, attempts to transform 4 to 3a by a 2-fold electrophilic cyclization via nitrogen-directed borylation on the benzene core were unsuccessful. One reason is, probably, attributed to the electron-poor benzene central core, which is unfavorable for electrophilic attack. In an improved approach, the key intermediate 2a with the trimethylsilyl (TMS) group as either leaving group or oriented group was then synthesized by an efficient Suzuki-Miyaura coupling reaction of 1,4-dibromo-2,5-bis(trimethylsilyl)benzene 1a with commercially available 2-aminophenylboronic acid pinacol ester. Afterward, upon the treatment of 2a with an excess amount of PhBCl₂ using triethylamine as catalyst in *o*-dichlorobenzene under 180 °C, compound 3a was readily obtained as a white crystalline powder in a very high yield (~90%). As far as we know, this is the first time TMS as a leaving group was used for stimulating borylation in the formation of BN-containing conjugated systems.

Alternatively, taking advantage of thieno[3,2-*b*]thiophene as the aromatic central core, the two position isomer intermediates 2b and 2c were achieved in good yields by the Suzuki cross-coupling of α - or β -substituted thieno[3,2-*b*]thiophene bromide with 2-aminophenylboronic acid pinacol ester, respectively. Upon treatment with PhBCl₂, 2b and 2c were easily transformed into the two targeted isomers 3b and 3c in

high yields of 87% and 90%, respectively. Similarly, BN-heteroacene on the basis of a larger aromatic core benzo[1,2-b:4,5-b']dithiophene **3d**, was achieved in 80% yield via the key intermediate **2d** under the same reaction conditions above. Apparently, these thiophene-based aromatic cores seem to be facile to undergo the 2-fold electrophilic borylation, even without the help of any leaving groups, probably due to their electron-rich characteristics associated with the thiophene moiety.

All of the new compounds were fully characterized by ^1H , ^{13}C NMR spectroscopy, and high-resolution mass spectrometry. The resonance peaks of the protons in the nitrogen site appear in the aromatic regions (at about 7.8–8.0 ppm, $\text{C}_2\text{D}_2\text{Cl}_4$, 298 K), suggesting the aromatic nature of these BN-heteroacenes. These compounds are stable against moisture and oxygen, even stored in air for several months without any obvious decomposition, as well as exhibiting good photostability under irradiation of 320 nm light. Thermogravimetric analysis (TGA) revealed their high decomposition temperature with a sequence of **3c** (440 °C) > **3b** (425 °C) > **3a** (360 °C) > **3d** (312 °C) (Figures S1–S4).

The structures of these compounds were further confirmed by X-ray crystallographic analysis (Figure 2). Single crystals of

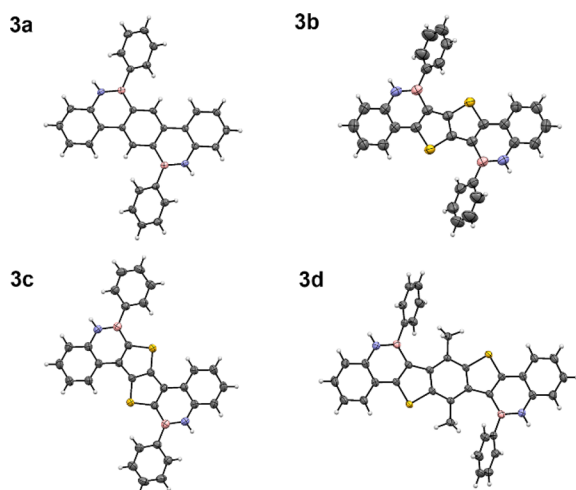


Figure 2. ORTEP drawings (50% probability for thermal ellipsoids) for compounds **3a–d**.

the compounds suitable for X-ray analysis were obtained by the slow evaporation of a chloroform solution for **3a** and an acetone solution for **3b** or **3d**. For compound **3c** with poor solubility, the single crystals were grown by slowly diffusing hexane into its saturated THF solution. Compounds **3a–c** show C_{2h} -symmetry structures with the relatively planar main backbones, as demonstrated by the largest dihedral angles of 1.4(4)°, 3.5(3)°, and 1.4(4)° among the fused rings, respectively. Whereas, compound **3d** adopts a slightly twisted conformation with the larger dihedral angles of 17.3(4)°, probably due to the steric repulsion between the methyl groups of the benzo[1,2-b:4,5-b']dithiophene core and phenyl rings attached on the boron atoms. The B–N bond lengths for compounds **3a–d** are 1.409(3)–1.416(3) Å, within the range of those for BN-heteroacenes, indicative of a typical double-bond character.^{16,19}

The crystal packing diagrams for **3a–d** are shown in Figure 3. The crystal of **3a** exhibits an edge-to-face herringbone-packing pattern. The alternating π -stacked columns are tilted at

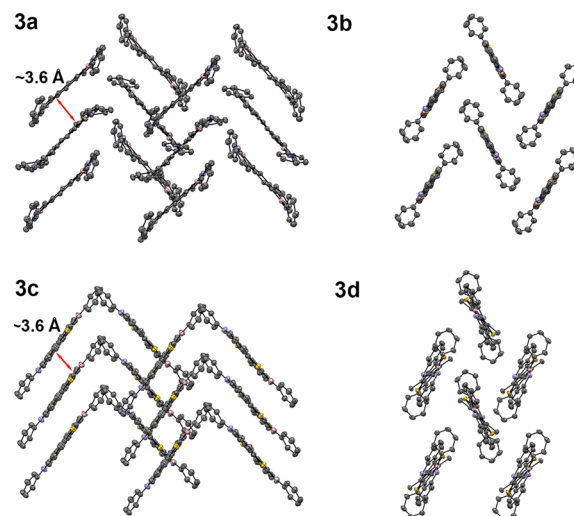


Figure 3. Crystal packing diagrams for compounds **3a–d**.

an angle of around 80°. In each of the π -stacked columns, the shortest distance of ~ 3.6 Å between the neighboring molecules manifests the significant π – π stacking interactions. The shortest distance between boron and nitrogen atoms from neighboring molecules is ~ 4.6 Å, revealing weak dipole–dipole interactions comparable with those of other azaborines (~ 6.7 Å).¹² Compound **3b** shows a herringbone packing motif consisting of slipped stacked columns tilted at an angle of $\sim 70^\circ$. The distance of the neighboring layers is ~ 3.9 Å, without the obvious face-to-face π – π stacking interactions observed. Interestingly, compound **3c** adopts a very similar packing pattern to that of compound **3a**, with alternating π -stacked columns tilted at an angle of around 80°, and the shortest distance between the neighboring molecules is ~ 3.6 Å, while the closest intermolecular BN dipole–dipole distance is enlarged to 4.9 Å. Similar to compound **3b**, the packing diagram of **3d** adopts a herringbone packing motif, in which the slipped stacked columns are tilted at a smaller angle of around 50°. However, there is no distinct face-to-face π – π stacking found in crystal packing, despite the fact that it possesses an extended π -conjugated backbone. These results demonstrate that the position isomerization or the fusion of the aromatic units in the molecular main backbones can remarkably alter the structural characteristics in solid state of the as-prepared BN-heteroacenes.

The absorption spectra of the as-prepared BN-heteroacenes feature vibronically split bands (Figure 4a), indicative of their rigid conjugated structures, in line with the crystallographic analyses. There are two strong absorption bands in the wavelength regions of 250–300 nm and 300–400 nm assigned to the π – π^* transitions. Compound **3a** shows three main absorption bands at around 250–300 nm and a series of weak absorption bands at around 300–390 nm. Such a profile is similar to the full-carbon analogue dibenz[*a,h*]anthracene.²⁰ Interestingly, the absorption profile of compound **3c**, completely different from that of its isomer **3b**, reveals a low-energy absorption maximum at 365 nm, with a blue shift of 18 nm as compared with that of $\lambda_{\text{max}} = 383$ nm in the latter case, indicating that coupling the lateral benzene rings via the α -carbon position of the thiophene moiety in the thienothiophene core for **3b** is much more favorable for the electron delocalization along the main backbone than that via β -carbon position for **3c**. Accordingly, **3b** and **3c** are bright yellow and

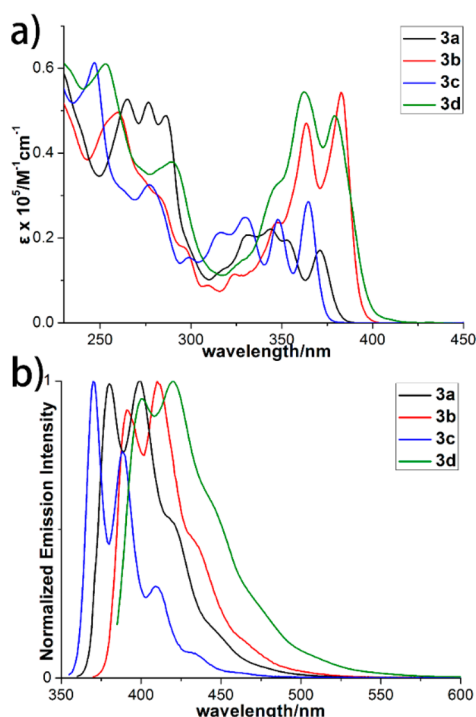


Figure 4. (a) UV-vis absorption spectra and (b) fluorescence emission spectra of 3a–d at 10^{-5} M in CH_2Cl_2 .

colorless in solid state, respectively (Figure S5). Compound 3d with seven fused aromatic rings in the main backbone is close to the reported polyarenes and heteroacenes with the longest conjugated lengths.²¹ However, the absorption bands in the low energy regions for 3d are slightly blue-shifted with respect to those of 3b, although the former one has an extended fused backbone with an annulated benzene ring in the internal position, which is contrasted to the results from the other heteroacenes or polyarenes.^{22,23} Such an unusual phenomenon is probably attributed to a declined planarity of the conjugated main backbone in the case of 3d, arising from the spatially intramolecular repulsion as shown in the single crystal analysis above.²⁴ Additionally, the main absorption bands of 3a–d in the thin films show broadening and red-shifts relative to those in solution, demonstrating their stronger intermolecular interactions in solid state (Figures S6–S9).

The fluorescence properties of these compounds were also investigated (Figure 4b and Table 1). Distinct blue shifts of the emission maxima were found in such a sequence: 3c (370 nm) < 3a (380 nm) < 3b (391 nm) < 3d (400 nm). The Stokes shifts were observed in the order 3c (370 cm^{-1}) < 3b (534 cm^{-1}) < 3a (638 cm^{-1}) < 3d (1385 cm^{-1}), reflecting their gradually increased geometric distortion between the ground

state and excited state, highly associated with their molecular rigidities depicted as single crystal analyses.²⁴ Further, 3a exhibits strong blue emission with a much higher quantum yield and longer fluorescence lifetime ($\Phi_{\text{PL}} = 0.50$ in solution, 0.22 in solid state; τ , 5.9 ns) than other three BN-heteroacenes. Strikingly, 3c offers remarkably declined luminescence quantum yield and fluorescent lifetime ($\Phi_{\text{PL}} = 0.04$ in solution, or <0.01 in solid state; τ , 0.7 ns) compared with its isomer 3b ($\Phi_{\text{PL}} = 0.25$ in solution, 0.11 in solid state; τ , 1.3 ns) while 3d also offers a very weak luminescent emission either in solution ($\Phi_{\text{PL}} = 0.02$) or in solid state ($\Phi_{\text{PL}} = 0.01$). Although, these phenomena are still unclear at this moment, the differences derived from the aromatic central cores definitely exert a strong influence on their geometric structures in excited state of these kinds of BN-heteroacenes.²⁵

The electrochemical behaviors of these BN-heteroacenes were investigated by cyclic voltammeteries (CVs), disclosing their irreversible oxidation processes without reduction waves under the measurement conditions (Figure 5 and Table 1).

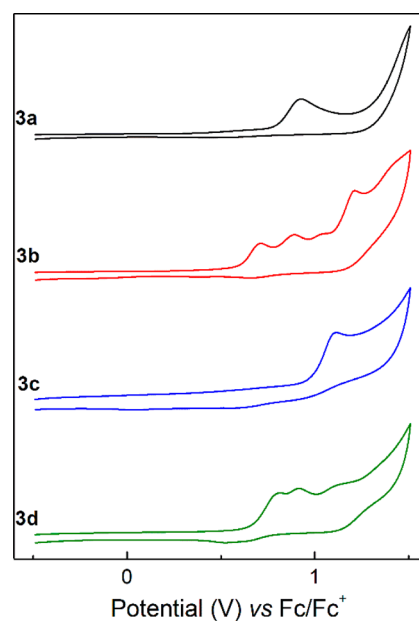


Figure 5. Cyclic voltammograms of compounds 3a–d measured in CH_2Cl_2 (0.1 mol/L $n\text{-Bu}_4\text{NPF}_6$) at a scan rate of 100 mV/s.

Their first oxidation potentials were observed in the following order: 3b < 3d < 3a < 3c. Accordingly, the HOMO energy levels of the as-prepared BN-heteroacenes were evaluated from the onsets of the first oxidation potential in a sequence of 3c (-5.78 eV) < 3a (-5.60 eV) < 3d (-5.46 eV) < 3b (-5.39 eV). It is noteworthy that several oxidation peaks were

Table 1. Photophysical and Electrochemical Data for BN-Heteroacenes 3a–d

	UV-vis absorption			fluorescence			electrochemistry ^c		calculation ^d	
	λ_{abs} (nm)	$\log \epsilon$	E_g^a (eV)	λ_{em} (nm)	Φ_{PL}^b	τ (ns)	HOMO (eV)	LUMO (eV)	HOMO (eV)	LUMO (eV)
3a	371	4.23	3.25	380, 399	0.50/0.22	5.9	-5.60	-2.35	-5.61	-1.56
3b	383	4.73	3.16	391, 410	0.25/0.11	1.3	-5.39	-2.23	-5.41	-1.72
3c	365	4.46	3.32	370	0.04/<0.01	0.7	-5.78	-2.46	-5.78	-1.89
3d	379	4.69	3.12	400, 420	0.02/0.01	0.6	-5.46	-2.34	-5.42	-1.81

^aEstimated from the UV-vis absorption edge. ^bAbsolute value, in solution and in solid. ^cCalculated from the onset of the first oxidation wave. HOMO = $-E_{\text{ox1}} - 4.80\text{ eV}$, LOMO = HOMO + E_g . ^dObtained by DFT calculations.

observed in the CV profiles of **3b** and **3d**, much clearly shown in their profiles of differential pulse voltammeters (DVPs) (Figure S14). Such phenomena could be attributed to the much larger π -conjugated systems of the two molecules, well in agreement with their molecular structure characteristics and optical properties aforementioned. The low-lying HOMO energy levels suggest that these compounds might be good candidates for air-stable p-type semiconductors.²⁶ Meanwhile, the molecular energy levels of the as-prepared BN-heteroacenes can be finely tuned through their fused-ring skeletons.

Finally, the density functional theory (DFT) calculations (RB3LYP/6-311G(d,p) level) of the BN-heteroacenes were performed (Figure 6 and Table 1). In the case of **3a**, the

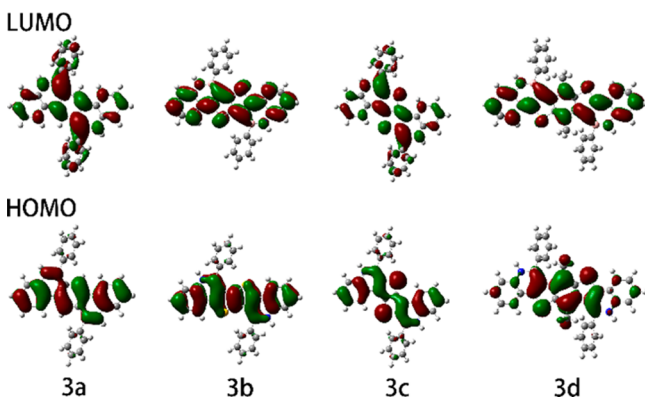


Figure 6. Calculated molecular orbitals of compounds **3a–d**. Corresponding energies and coordinates are provided in the Supporting Information.

HOMO is confined on the rigid backbone, while the LUMO is delocalized over the whole molecule including the side phenyl groups. Compound **3b** shows an almost flat backbone, with HOMO and LUMO located over the entire rigid main backbone, which demonstrates its fully π -conjugated system. However, for its isomer **3c**, its HOMO and LUMO orbits only occupy the parts of the main backbone. Surprisingly, for compound **3d**, the HOMO is mainly confined on the benzodithiophene core, partially involving the bilateral BN-embedded naphthalene moieties, while the LUMO occupies the full backbone scaffold. These theoretical results are well in support of the aforementioned experimental analyses.

CONCLUSIONS

In summary, a series of C_{2h} -symmetric BN-heteroacenes with two boron atoms attached on the different aromatic central cores have been successfully synthesized through 2-fold successive electrophilic borylation on one central core. For the first time, we took advantage of TMS as either leaving group or oriented group for efficiently improving the preparation of BN-embedded PAHs. Such a strategy would allow for the construction of BN-containing conjugated systems with much complex structural features. The physical properties of the as-synthesized BN-heteroacenes in either solid state or solution, can be finely tuned through the position isomerization or the fused ring numbers of the aromatic central core. Attempts to fabricate various electronic devices, such as OLEDs, by using these molecules as active components, are in progress.

EXPERIMENTAL SECTION

General Information. 1,4-Dibromo-2,5-bis(trimethylsilyl)-benzene,²⁷ 2,5-dibromothieno[3,2-*b*]thiophene,²⁸ and 4,8-dimethylbenzo[1,2-*b*:4,5-*b'*]dithiophene^{29,30} were prepared using literature methods. 3,6-Dibromothieno[3,2-*b*]thiophene was purchased from a chemical supplier. The reactions were performed using standard vacuum-line and Schlenk techniques, and workup and purification of all compounds were performed under air and with reagent-grade solvents.

¹H and ¹³C NMR spectra were referenced to residual signals of the deuterated solvent. ¹¹B spectra were externally referenced to BF₃·Et₂O (0 ppm). High-resolution electrospray ionization mass spectrometry was performed on a QToF spectrometer. Thermogravimetric analysis (TGA) was measured with a heating rate of 10 °C min⁻¹ under flowing N₂. CV was performed in anhydrous dichloromethane containing recrystallized tetra-*n*-butyl-ammoniumhexafluorophosphate (TBAPF6, 0.1M) as supporting electrolyte at 298 K. A conventional three electrode cell was used with a platinum working electrode (surface area of 0.3 mm²) and a platinum wire as the counter electrode. The Pt working electrode was routinely polished with a polishing alumina suspension and rinsed with acetone before use. The measured potentials were recorded with respect to the Ag/AgCl reference electrode. All electrochemical measurements were carried out under an atmospheric pressure of nitrogen. Geometry optimizations and the analysis of HOMOs and LUMOs were performed at the DFT level (RB3LYP/6-311G(d,p)). The initial structures were determined by X-ray diffraction analyses. All calculations were performed using Gaussian 09, rev. A02.³¹

1,4-Dibromo-2,5-bis(trimethylsilyl)benzene (1a). LDA (2 M, 55 mL, 110 mmol) was added dropwise to the suspension of 1,4-dibromobenzene (11.8 g, 50 mmol) in THF (100 mL) containing TMSCl (12.0 g, 14 mL) at -78 °C. The resultant orange solution was kept at -78 °C for 1 h and then allowed to come to room temperature. The reactant was hydrolyzed with dilute sulfuric acid solution. The yellow organic phase was separated, and the water phase was extracted with ether three times. Evaporation of the combined organic solutions left the crude product as a pale yellow solid residue. It was filtered, washed with cold methanol, and dried to give **1a** as a white crystalline material (15 g, 79%). mp = 97–99 °C; ¹H NMR (400 MHz, CDCl₃) δ 7.50 (s, 2H), 0.38 (s, 18H); ¹³C NMR (101 MHz, CDCl₃) δ 144.8, 140.0, 129.5, -0.7. No signal was detected in HRMS using acetonitrile as the solvent.

2,5-Dibromothieno[3,2-*b*]thiophene (1b). To a well-stirred solution of thieno[3,2-*b*]thiophene (3.5 g, 25 mmol) in CHCl₃ (75 mL) was added NBS (8.9 g, 50 mmol) dissolved in DMF (50 mL) dropwise at 0 °C in the absence of light. The mixture was allowed to warm to room temperature slowly. After stirring for 12 h, the reaction was quenched with ice, and the aqueous phase was extracted with dichloromethane three times. The combined organic layers were then washed several times with brine and dried over magnesium sulfate afterward. The solvent was removed under reduced pressure to give **1b** as pale yellow flakes (7.0 g, 94% yield). The product should be kept at -20 °C in a refrigerator; otherwise, it will be soon decompose to a black solid. mp = 115–117 °C; ¹H NMR (400 MHz, CDCl₃) δ 7.18 (s, 2H); ¹³C NMR (101 MHz, CDCl₃) δ 138.4, 121.9, 113.7. MALDI-TOF(*m/z*): calcd for C₆H₂Br₂S₂ [M]⁺ 297.79; found, 297.48. No signal was detected in HRMS using acetonitrile as the solvent.

2,6-Dibromo-4,8-dimethylbenzo[1,2-*b*:4,5-*b'*]dithiophene (1d). In a dry two-necked flask, benzo[1,2-*b*:4,5-*b'*]dithiophene-4,8-dione (5.5 g, 25 mmol) was dissolved in freshly distilled THF (150 mL). To this stirred suspension, a solution of MeLi in hexane (80 mmol, 1–2 M) was added dropwise over 10 min at room temperature. The mixture was stirred for 2 h under reflux conditions, cooled down, and then quenched with 6 mL of water. SnCl₂·2H₂O (25 g, 105 mmol) in 50 mL of HCl was then added with stirring. The mixture was refluxed overnight, and after cooling down, it was quenched with brine. The organic phase was separated, and the aqueous phase was extracted with hexane three times. The organic phases were combined, dried with magnesium sulfate, and concentrated using rotary evaporation. The

crude product was purified by chromatography on silica gel (petroleum ether) to give the product 4,8-dimethylbenzo[1,2-*b*:4,5-*b'*]dithiophene as a light yellow powder (2.0 g, 22%). mp = 148–150 °C; $^1\text{H NMR}$ (400 MHz, CDCl_3) δ 7.48 (q, $J = 5.6$ Hz, 4H), 2.82 (s, 6H); $^{13}\text{C NMR}$ (101 MHz, CDCl_3) δ 137.7, 136.2, 126.1, 123.6, 122.1, 18.2. MALDI-TOF(m/z): calcd for $\text{C}_{12}\text{H}_{10}\text{S}_2$ [M^+] 218.02; found, 217.81. No signal was detected in HRMS using acetonitrile as the solvent.

To a well-stirred solution of 4,8-dimethylbenzo[1,2-*b*:4,5-*b'*]dithiophene (874 mg, 4.0 mmol) in CH_2Cl_2 (30 mL) and acetic acid (7.5 mL) in a two-necked flask under an argon atmosphere was slowly added NBS (1.43 g, 8.0 mmol) in the absence of light. The resulting mixture was stirred at room temperature overnight. The reactant was poured into brine, extracted once by dichloromethane, and the solvent was evaporated in vacuo. The crude product was washed with water and methanol several times to provide product **1d** (1.2 g, 80% yield) as a green powder after drying in vacuo. $^1\text{H NMR}$ (400 MHz, CDCl_3) δ 7.43 (s, 2H), 2.64 (s, 6H); $^{13}\text{C NMR}$ (101 MHz, CDCl_3) δ 139.0, 135.8, 125.1, 122.2, 115.1, 17.9. MALDI-TOF(m/z): calcd for $\text{C}_{12}\text{H}_8\text{Br}_2\text{S}_2$ [M^+] 375.84; found, 375.41. No signal was detected in HRMS using acetonitrile as the solvent.

General Procedure A for the Dianiline Precursors: Representative Procedure for the Synthesis of 2,2'-(1,4-Bis(trimethylsilyl)benzene-2,5-diyl)dianiline (2a). In a 200 mL long-necked Schlenk flask, 1,4-dibromo-2,5-bis(trimethylsilyl)benzene **1a** (760 mg, 2.0 mmol) and 2-(4,4,5,5-tetramethyl-1,3,2-dioxaborolan-2-yl)benzenamine (1.31 g, 6.0 mmol) were charged under the protection of argon. After adding 80 mL of dimethoxyethane and 20 mL of NaHCO_3 aqueous solution (1.0 mol/L), the mixture was degassed for 30 min. $\text{Pd}(\text{PPh}_3)_4$ (230 mg, 0.20 mmol) was added, then the mixture was heated to 90 °C and stirred for 24 h. The reactant was poured into brine and extracted by dichloromethane several times. The organic phase was dried over magnesium sulfate, and the solvent was evaporated in vacuo. The crude product was purified by silica chromatography.

2,2'-(1,4-Bis(trimethylsilyl)benzene-2,5-diyl)dianiline (**2a**). The title compound was purified by silica chromatography (CH_2Cl_2) to give the product as a white powder (780 mg, 92%). $^1\text{H NMR}$ (400 MHz, CDCl_3) δ 7.48 (d, $J = 8.6$ Hz, 2H), 7.19 (td, $J = 7.7, 1.5$ Hz, 2H), 7.08–7.04 (m, 2H), 6.85–6.72 (m, 4H), 3.56 (br, 4H), 0.00 (t, $J = 1.3$ Hz, 18H); $^{13}\text{C NMR}$ (101 MHz, CDCl_3) δ 144.6, 144.4, 143.5, 143.4, 141.1, 136.7, 131.2, 131.1, 129.7, 128.7, 117.8, 117.7, 115.1, 115.0, 0.1. HRMS (ESI, m/z): calcd for $\text{C}_{24}\text{H}_{33}\text{N}_2\text{Si}_2$ [M^+] 405.2177; found, 405.2178.

2,2'-(Thieno[3,2-*b*]thiophene-2,5-diyl)dianiline (**2b**). Prepared following general procedure A using 2,5-dibromo-thieno[3,2-*b*]thiophene **1b** (600 mg, 2.0 mmol) as starting material and purified by silica chromatography (CH_2Cl_2) to give the product as a pale yellow powder (520 mg, 81%). $^1\text{H NMR}$ (400 MHz, CDCl_3) δ 7.38 (s, 2H), 7.33 (dd, $J = 7.6, 1.4$ Hz, 2H), 7.18 (td, $J = 7.8, 1.5$ Hz, 2H), 6.85–6.78 (m, 4H), 4.07 (br, 4H); $^{13}\text{C NMR}$ (101 MHz, CDCl_3) δ 144.4, 142.7, 139.4, 131.1, 129.6, 120.3, 118.8, 118.4, 116.2. HRMS (ESI, m/z): calcd for $\text{C}_{18}\text{H}_{15}\text{N}_2\text{S}_2$ [M^+] 323.0671; found, 323.0665.

2,2'-(Thieno[3,2-*b*]thiophene-3,6-diyl)dianiline (**2c**). Prepared following general procedure A using 3,6-dibromo-thieno[3,2-*b*]thiophene **1c** (596 mg, 2.0 mmol) as starting material and purified by silica chromatography (CH_2Cl_2) to give the product as a brown powder (580 mg, 89%). $^1\text{H NMR}$ (400 MHz, CDCl_3) δ 7.48 (s, 2H), 7.42 (dd, $J = 7.6, 1.6$ Hz, 2H), 7.22 (td, $J = 7.7, 1.5$ Hz, 2H), 6.89–6.82 (m, 4H), 3.95 (br, 4H); $^{13}\text{C NMR}$ (101 MHz, CDCl_3) δ 144.3, 139.8, 132.5, 129.9, 129.3, 125.0, 120.5, 118.7, 116.1. HRMS (ESI, m/z): calcd for $\text{C}_{18}\text{H}_{15}\text{N}_2\text{S}_2$ [M^+] 323.0671; found, 323.0687.

2,2'-(4,8-Dimethylbenzo[1,2-*b*:4,5-*b'*]dithiophene-2,6-diyl)dianiline (**2d**). Prepared following general procedure A using 2,6-dibromo-4,8-dimethylbenzo[1,2-*b*:4,5-*b'*]dithiophene **1d** (750 mg, 2.0 mmol) as starting material and purified by silica chromatography (CH_2Cl_2 /petroleum ether = 1:1) to give the product as a green powder (480 mg, 64%). $^1\text{H NMR}$ (400 MHz, CDCl_3) δ 7.58 (s, 2H), 7.43 (dd, $J = 7.6, 1.5$ Hz, 2H), 7.20 (td, $J = 7.8, 1.5$ Hz, 2H), 6.89–6.80

(m, 4H), 4.18 (s, 4H), 2.80 (s, 6H); $^{13}\text{C NMR}$ (101 MHz, CDCl_3) δ 144.4, 141.1, 137.8, 136.9, 131.2, 129.6, 123.3, 120.9, 120.4, 118.8, 116.2, 18.2. HRMS (ESI, m/z): calcd for $\text{C}_{24}\text{H}_{21}\text{N}_2\text{S}_2$ [M^+] 401.1146; found, 401.1150.

General Procedure B for BN-Heteroacenes: Representative Procedure for the Synthesis of BN-Dibenz[*a,h*]anthracene (3a).

To a solution of 2,2'-(1,4-bis(trimethylsilyl)benzene-2,5-diyl)dianiline (405 mg, 1.0 mmol) in *o*-dichlorobenzene (20 mL) under argon was added triethylamine (600 mg, 0.9 mL, 6.0 mmol) and phenyl-dichloroborane (480 mg, 0.4 mL, 3.0 mmol). The reaction mixture was heated to 180 °C for 12 h. After cooling to room temperature, the solvent was evaporated through reduced pressure distillation. The residue was then washed with methanol and then purified by flash chromatography on silica gel.

BN-Dibenz[*a,h*]anthracene (**3a**). The title compound was purified by silica chromatography (CH_2Cl_2 /petroleum ether = 1:2) to give the product as a white powder (390 mg, 90%). $^1\text{H NMR}$ (400 MHz, $\text{C}_2\text{D}_4\text{Cl}_2$) δ 9.40 (s, 2H), 8.49 (d, $J = 8.0$ Hz, 2H), 7.97 (d, $J = 6.4$ Hz, 4H), 7.84 (s, 2H), 7.70–7.58 (m, 6H), 7.49 (t, $J = 7.5$ Hz, 2H), 7.33 (dd, $J = 15.1, 7.6$ Hz, 4H); $^{13}\text{C NMR}$ (101 MHz, $\text{C}_2\text{D}_4\text{Cl}_2$) δ 139.2, 138.5, 135.9, 133.6, 133.3, 130.2, 129.0, 128.3, 128.2, 124.1, 123.4, 122.0, 119.2; $^{11}\text{B NMR}$ (128 MHz, CDCl_3) δ 37.27. HRMS (ESI, m/z): calcd for $\text{C}_{30}\text{H}_{23}\text{B}_2\text{N}_2$ [M^+] 433.2052; found, 433.2047.

BN-Dinaphthothienothiophene (**3b**). Prepared following general procedure B using 2,2'-(thieno[3,2-*b*]thiophene-2,5-diyl)dianiline **2b** (320 mg, 1.0 mmol) as the precursor and purified by silica chromatography (CH_2Cl_2 /petroleum ether = 1:1) to give the product as a bright yellow powder (430 mg, 87%). $^1\text{H NMR}$ (700 MHz, $\text{C}_2\text{D}_2\text{Cl}_4$) δ 8.01 (t, $J = 6.6$ Hz, 6H), 7.95 (s, 2H), 7.71–7.59 (m, 6H), 7.47 (t, $J = 7.2$ Hz, 2H), 7.41 (d, $J = 7.8$ Hz, 2H), 7.28 (t, $J = 7.4$ Hz, 2H); $^{13}\text{C NMR}$ (126 MHz, $\text{C}_2\text{D}_2\text{Cl}_4$, 373 K) δ 154.4, 141.9, 137.8, 132.5, 129.1, 128.1, 127.8, 124.5, 122.2, 121.8, 118.7; $^{11}\text{B NMR}$ (128 MHz, CDCl_3) δ 34.04. HRMS (ESI, m/z): calcd for $\text{C}_{30}\text{H}_{20}\text{B}_2\text{N}_2\text{S}_2$ [M^+] 492.1327; found, 492.1312.

BN-Dinaphthothienothiophene (**3c**). Prepared following general procedure B using 2,2'-(thieno[3,2-*b*]thiophene-3,6-diyl)dianiline **2c** (323 mg, 1.0 mmol) as the precursor and purified by sublimation because of the poor solubility to give the product as a white powder (450 mg, 90%). $^1\text{H NMR}$ (400 MHz, $\text{THF-}d_8$) δ 9.80 (s, 2H), 8.58 (d, $J = 7.9$ Hz, 2H), 8.24–8.14 (m, 4H), 7.76 (d, $J = 8.0$ Hz, 2H), 7.60–7.48 (m, 8H), 7.45 (t, $J = 7.5$ Hz, 2H); $^{13}\text{C NMR}$ (101 MHz, $\text{THF-}d_8$) δ 143.5, 140.9, 139.4, 134.2, 130.1, 128.7, 128.2, 126.0, 122.2, 121.7, 120.0. $^{11}\text{B NMR}$ (128 MHz, $\text{THF-}d_8$) δ 34.79; HRMS (ESI, m/z): calcd for $\text{C}_{30}\text{H}_{21}\text{B}_2\text{N}_2\text{S}_2$ [M^+] 493.1399; found, 493.1385.

BN-Dinaphthobenzodithiophene (**3d**). Prepared following general procedure B using 2,2'-(4,8-dimethylbenzo[1,2-*b*:4,5-*b'*]dithiophene-2,6-diyl)dianiline **2d** (400 mg, 1.0 mmol) as the precursor and purified by silica chromatography (CH_2Cl_2 /petroleum ether = 1:2) to give the product as a green powder (460 mg, 80%). $^1\text{H NMR}$ (700 MHz, $\text{C}_2\text{D}_2\text{Cl}_4$) δ 8.09 (d, $J = 7.9$ Hz, 2H), 7.92 (s, 2H), 7.71 (dd, $J = 6.3, 2.9$ Hz, 4H), 7.53 (t, $J = 7.0$ Hz, 2H), 7.50–7.48 (m, 6H), 7.41 (d, $J = 8.0$ Hz, 2H), 7.32 (t, $J = 7.4$ Hz, 2H); $^{13}\text{C NMR}$ (176 MHz, $\text{C}_2\text{D}_2\text{Cl}_4$) δ 153.9, 143.5, 139.7, 139.4, 138.2, 133.0, 131.7, 128.9, 128.4, 128.1, 125.8, 125.5, 121.8, 121.1, 118.4, 23.3; $^{11}\text{B NMR}$ (128 MHz, CDCl_3) δ 35.01. HRMS (ESI, m/z): calcd for $\text{C}_{36}\text{H}_{26}\text{B}_2\text{N}_2\text{S}_2$ [M^+] 570.1796; found, 570.1774.

■ ASSOCIATED CONTENT

Supporting Information

The Supporting Information is available free of charge on the ACS Publications website at DOI: 10.1021/acs.joc.5b01718.

TGA spectra, optical spectra, NMR spectra, computational details, coordinates, and energies of stationary points (PDF)

Single-crystal X-ray diffraction data (CIF)

■ AUTHOR INFORMATION

Corresponding Author

*E-mail: fan-zhang@sjtu.edu.cn

Notes

The authors declare no competing financial interest.

■ ACKNOWLEDGMENTS

We are grateful to Merck KGaA for financial support. We also acknowledge funding support from the Natural Science Foundation of China (NSFC 21174083) and the Shanghai Committee of Science and Technology (15JC1490500). We thank Dr. Xiaoli Zhao (East China Normal University) and Dr. Schollmeyer (University of Mainz) for X-ray crystal structure analysis.

■ REFERENCES

- (1) Anthony, J. E. *Chem. Rev.* **2006**, *106*, 5028–5048.
- (2) Wu, W.; Liu, Y.; Zhu, D. *Chem. Soc. Rev.* **2010**, *39*, 1489–1502.
- (3) Takimiya, K.; Shinamura, S.; Osaka, I.; Miyazaki, E. *Adv. Mater.* **2011**, *23*, 4347–4370.
- (4) Payne, M. M.; Parkin, S. R.; Anthony, J. E. *J. Am. Chem. Soc.* **2005**, *127*, 8028–8029.
- (5) Mondal, R.; Adhikari, R. M.; Shah, B. K.; Neckers, D. C. *Org. Lett.* **2007**, *9*, 2505–2508.
- (6) Payne, M. M.; Odom, S. A.; Parkin, S. R.; Anthony, J. E. *Org. Lett.* **2004**, *6*, 3325–3328.
- (7) Niimi, K.; Shinamura, S.; Osaka, I.; Miyazaki, E.; Takimiya, K. *J. Am. Chem. Soc.* **2011**, *133*, 8732–8739.
- (8) Mori, T.; Nishimura, T.; Yamamoto, T.; Doi, I.; Miyazaki, E.; Osaka, I.; Takimiya, K. *J. Am. Chem. Soc.* **2013**, *135*, 13900–13913.
- (9) Liu, Z.; Marder, T. B. *Angew. Chem., Int. Ed.* **2008**, *47*, 242–244.
- (10) Bosdet, M. J. D.; Piers, W. E. *Can. J. Chem.* **2009**, *87*, 8–29.
- (11) Campbell, P. G.; Marwitz, A. J. V.; Liu, S.-Y. *Angew. Chem., Int. Ed.* **2012**, *51*, 6074–6092.
- (12) Wang, X.-Y.; Lin, H. R.; Lei, T.; Yang, D. C.; Zhuang, F. D.; Wang, J. Y.; Yuan, S. C.; Pei, J. *Angew. Chem., Int. Ed.* **2013**, *52*, 3117–3120.
- (13) Wang, X.-Y.; Zhuang, F. D.; Wang, R. B.; Wang, X. C.; Cao, X. Y.; Wang, J. Y.; Pei, J. *J. Am. Chem. Soc.* **2014**, *136*, 3764–3767.
- (14) Hashimoto, S.; Ikuta, T.; Shiren, K.; Nakatsuka, S.; Ni, J. P.; Nakamura, M.; Hatakeyama, T. *Chem. Mater.* **2014**, *26*, 6265–6271.
- (15) Wang, X.-Y.; Narita, A.; Feng, X.; Müllen, K. *J. Am. Chem. Soc.* **2015**, *137*, 7668–7671.
- (16) Wang, X.; Zhang, F.; Liu, J.; Tang, R.; Fu, Y.; Wu, D.; Xu, Q.; Zhuang, X.; He, G.; Feng, X. *Org. Lett.* **2013**, *15*, 5714–5717.
- (17) Chissick, S. S.; Dewar, M. J. S.; Maitlis, P. M. *Tetrahedron Lett.* **1960**, *1*, 8–10.
- (18) Hatakeyama, T.; Hashimoto, S.; Seki, S.; Nakamura, M. *J. Am. Chem. Soc.* **2011**, *133*, 18614–18617.
- (19) Lepeltier, M.; Lukyanova, O.; Jacobson, A.; Jeeva, S.; Perepichka, D. F. *Chem. Commun.* **2010**, *46*, 7007–7009.
- (20) Umeda, R.; Miyake, S.; Nishiyama, Y. *Chem. Lett.* **2012**, *41*, 215–217.
- (21) Xiao, J.; Duong, H. M.; Liu, Y.; Shi, W.; Ji, L.; Li, G.; Li, S.; Liu, X.-W.; Ma, J.; Wudl, F.; Zhang, Q. *Angew. Chem., Int. Ed.* **2012**, *51*, 6094–6098.
- (22) Schmidt, W. *J. Chem. Phys.* **1977**, *66*, 828–845.
- (23) Dias, J. R. *Handbook of Polycyclic Hydrocarbons. Part A: Benzenoid Hydrocarbons*; Elsevier Science, Ltd.: New York, 1987; p 388.
- (24) Jaska, C. A.; Emslie, D. J. H.; Bosdet, M. J. D.; Piers, W. E.; Sorensen, T. S.; Parvez, M. *J. Am. Chem. Soc.* **2006**, *128*, 10885–10896.
- (25) Suzuki, Y.; Okamoto, T.; Wakamiya, A.; Yamaguchi, S. *Org. Lett.* **2008**, *10*, 3393–3396.
- (26) Gao, J. H.; Li, R. J.; Li, L. Q.; Meng, Q.; Jiang, H.; Li, H. X.; Hu, W. P. *Adv. Mater.* **2007**, *19*, 3008–3011.
- (27) Luliński, S.; Serwatowski, J. *J. Org. Chem.* **2003**, *68*, 5384–5387.
- (28) Zhong, H.; Li, Z.; Deledalle, F.; Fregoso, E. C.; Shahid, M.; Fei, Z.; Nielsen, C. B.; Yaacobi-Gross, N.; Rossbauer, S.; Anthopoulos, T. D. *J. Am. Chem. Soc.* **2013**, *135*, 2040–2043.
- (29) Pappenfus, T. M.; Seidenkranz, D. T.; Reinheimer, E. W. *Heterocycles* **2012**, *85*, 355–364.
- (30) Pan, H.; Li, Y.; Wu, Y.; Liu, P.; Ong, B. S.; Zhu, S.; Xu, G. *J. Am. Chem. Soc.* **2007**, *129*, 4112–4113.
- (31) Frisch, M. J.; Trucks, G. W.; Schlegel, H. B.; Scuseria, G. E.; Robb, M. A.; Cheeseman, J. R.; Scalmani, G.; Barone, V.; Mennucci, B.; Petersson, G. A.; Nakatsuji, H.; Caricato, M.; Li, X.; Hratchian, H. P.; Izmaylov, A. F.; Bloino, J.; Zheng, G.; Sonnenberg, J. L.; Hada, M.; Ehara, M.; Toyota, K.; Fukuda, R.; Hasegawa, J.; Ishida, M.; Nakajima, T.; Honda, Y.; Kitao, O.; Nakai, H.; Vreven, T.; Montgomery, J. A., Jr.; Peralta, J. E.; Ogliaro, F.; Bearpark, M.; Heyd, J. J.; Brothers, E.; Kudin, K. N.; Staroverov, V. N.; Kobayashi, R.; Normand, J.; Raghavachari, K.; Rendell, A.; Burant, J. C.; Iyengar, S. S.; Tomasi, J.; Cossi, M.; Rega, N.; Millam, J. M.; Klene, M.; Knox, J. E.; Cross, J. B.; Bakken, V.; Adamo, C.; Jaramillo, J.; Gomperts, R.; Stratmann, R. E.; Yazyev, O.; Austin, A. J.; Cammi, R.; Pomelli, C.; Ochterski, J. W.; Martin, R. L.; Morokuma, K.; Zakrzewski, V. G.; Voth, G. A.; Salvador, P.; Dannenberg, J. J.; Dapprich, S.; Daniels, A. D.; Farkas, O.; Foresman, J. B.; Ortiz, J. V.; Cioslowski, J.; Fox, D. J. *Gaussian 09*, revision A.02; Gaussian, Inc.: Wallingford, CT, 2009.